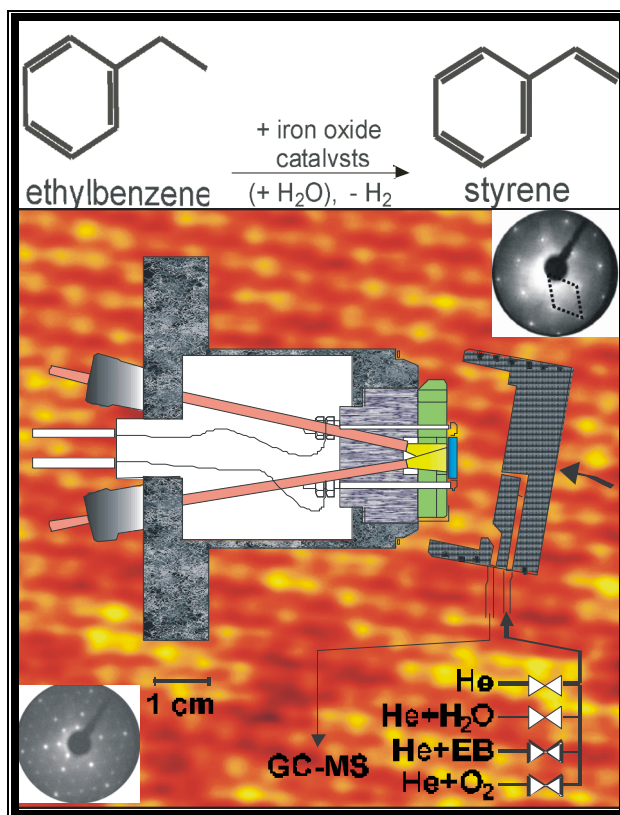


*Styrene synthesis:*  
*In-situ Characterization and Reactivity*  
*Measurements over Unpromoted and*  
*Potassium Promoted Iron Oxide Model*  
*Catalysts*



By

*Osama Shekhah*

**Styrene synthesis:  
In-situ Characterization and Reactivity  
Measurements over Unpromoted and Potassium  
Promoted Iron Oxide Model Catalysts**

Inaugural-Dissertation

zur Erlangung des Grades

**Doktor der Naturwissenschaften**

Am Fachbereich Biologie, Chemie, Pharmazie

Der Freien Universität Berlin

Vorgelegt in englischer Sprache

von

Osama Shekhah

Aus Jordanien

Berlin 2004

**Gutachter:**

**Prof. Dr. R. Schlögl**

Fritz Haber Institute der MPG  
Abt. Anorganische Chemie  
Faradayweg 4-6  
14195 Berlin

**Prof. Dr. K. Christmann**

Freie Universität Berlin  
Fachbereich Biologie, Chemie, Pharmazie  
Institut für Chemie-Physikalische und Theoretische Chemie  
Takustr. 3  
14195 Berlin

Tag der Prüfung: 06. Mai. 2004

## Contents

### Chapter-1: Introduction (styrene synthesis)

1.1	History .....	2
1.2	Reaction thermodynamics .....	3
1.3	Reaction kinetics and mechanism .....	5
1.4	Industrial catalysts composition.....	6
1.5	Catalyst deactivation.....	8
1.5.1	Coke deposition.....	9
1.5.2	Loss or redistribution of promoters.....	9
1.5.3	Oxidation state.....	11
1.5.4	Physical degradation .....	11
1.6	Alternative processes for styrene St synthesis (oxidative dehydrogenation of EB).....	12

### Chapter-2 Iron oxide model catalysts: A surface science approach to styrene synthesis

2.1	Introduction .....	15
2.2	Preparation and characterization of iron oxide thin films.....	16
2.2.1	Geometric surface structures and stability ranges of iron oxides.....	16
2.2.2	Potassium iron oxide compounds: Structure and stability ranges .....	21
2.3	Surface and structure Characterization .....	23
2.3.1	LEED and STM.....	23
2.3.2	AES measurements.....	26
2.3.3	Adsorption properties (TDS, UPS and NEXAFS).....	28
2.3.4	Low and medium pressure reactivity measurements.....	30
2.4	Aims and work strategy.....	33

### Chapter-3 Experimental

3.1	Instrumentation setup.....	36
3.1.1	UHV analysis system.....	36
3.1.2	Sample transfer and heating.....	37
3.1.3	High pressure reaction cells.....	39
3.1.4	The reactor.....	40
3.1.5	The laser heating system.....	42
3.1.6	The gas supply system.....	42
3.2	Spectroscopic and microscopic characterization methods.....	44
3.2.1	LEED, TPO and AES.....	44
3.3	Preparation of epitaxial iron oxide thin films.....	44

3.4	Pressed powder samples of unpromoted Fe <sub>2</sub> O <sub>3</sub> .....	46
3.4.1	Preparation of the pressed powder samples .....	46
3.4.2	Characterization of the pressed powder samples (BET, XRD and SEM-EDX).....	47
3.4.3	Cleaning of the pressed powder samples.....	48
3.4	Reaction experiments.....	48
<b>Chapter 4 Results</b>		
4.1	Blank reactivity experiments.....	52
4.2	Unpromoted model catalysts .....	52
4.2.1	Dehydrogenation reaction on Fe <sub>2</sub> O <sub>3</sub> (0001) and Fe <sub>3</sub> O <sub>4</sub> (111) model catalysts in presence of steam(normal conditions).....	52
4.2.2	Dehydrogenation reaction on Fe <sub>2</sub> O <sub>3</sub> (0001) model catalysts without steam (reductive conditions).....	57
4.2.3	Dehydrogenation reaction on Fe <sub>2</sub> O <sub>3</sub> (0001) model catalysts in presence of steam and oxygen (oxidative conditions).....	59
4.2.4	Dehydrogenation reaction on Fe <sub>2</sub> O <sub>3</sub> (0001) model catalysts in presence of steam and oxygen, effect of oxygen concentration on the activity.....	61
4.2.5	Dehydrogenation reaction on Fe <sub>2</sub> O <sub>3</sub> (0001) model catalysts in presence of steam. Oxygen on and off experiments .....	63
4.2.6	Dehydrogenation reaction on Fe <sub>2</sub> O <sub>3</sub> (0001) model catalysts in presence of steam and oxygen at different temperatures.....	65
4.3	Promoted iron oxide (KFe <sub>x</sub> O <sub>y</sub> ) model catalysts .....	65
4.3.1	Dehydrogenation reaction on KFe <sub>x</sub> O <sub>y</sub> model catalysts in presence of steam (normal conditions), effect of potassium content.....	67
4.3.2	Carbon formation from reaction on KFe <sub>x</sub> O <sub>y</sub> promoted and unpromoted catalysts (normal conditions).....	70
4.3.3	The effect of reactivation with steam on the dehydrogenation reaction on potassium promoted (KFe <sub>x</sub> O <sub>y</sub> ) model catalysts.....	71
4.3.4	Dehydrogenation reaction on KFe <sub>x</sub> O <sub>y</sub> model catalysts in presence of steam and oxygen (oxidative conditions).....	74
4.3.5	Dehydrogenation reaction on KFe <sub>x</sub> O <sub>y</sub> model catalysts without steam (reductive conditions), effect of potassium promoting on the reduction of the catalyst.....	76

4.3.6	Dehydrogenation reaction on $\text{KFe}_x\text{O}_y$ model catalysts in presence of steam. Oxygen on off experiments.....	78
4.3.7	Dehydrogenation reaction on $\text{KFe}_x\text{O}_y$ model catalysts in presence of steam and oxygen, effect of oxygen concentration ...	78
4.3.8	Dehydrogenation reaction on $\text{KFe}_x\text{O}_y$ model catalysts in presence of steam and oxygen at different reaction temperatures. ....	80
4.4	Pressed hematite ( $\text{Fe}_2\text{O}_3$ ) powder samples	
4.4.1	Reaction on pressed powder samples in fixed bed reactor .....	81
4.4.2	Reaction on pressed powder samples in micro flow reactor .....	82
	a) Reaction in the presence of EB and steam in the feed. ....	85
	b) Reaction in the presence of EB, steam and oxygen in the feed.....	92
<b>Chapter-5 Discussion</b>		
5.1	Unpromoted model catalyst.....	98
5.2	Promoted model catalyst.....	103
5.3	Pressed powder samples.....	114
5.4	Reaction model and mechanism.....	116
5.5	Conclusions.....	119
<b>References</b>		
<b>Acknowledgement</b>		
<b>Curriculum vita</b>		
<b>Abstracts</b>		

## Acronyms

<b>AES</b>	Auger-Electron Spectroscopy
$E_{ads}$	Adsorption energy
<b>EDX</b>	Energy Dispersive X-ray Emission Analysis
<b>EB</b>	Ethylbenzene
<b>St</b>	Styrene
<b>fcc</b>	face centered cubic
<b>FID</b>	Flame Ionization Detector
<b>hcp</b>	hexagonal close packed
<b>ISS</b>	Ion Scattering Spectroscopy
$k_i$	rate constant
<b>K</b>	Equilibrium constant
<b>LEED</b>	Low-Energy Electron Diffraction
<b>ML</b>	monolayer
$n$	frequency factor
<b>NEXAFS</b>	Near-Edge X-ray Absorption Fine Structure
<b>p</b>	gas pressure
<b>PEEM</b>	Photoelectron Emission Spectroscopy
$q_{st}$	Isosteric heat of adsorption
<b>r</b>	Reaction rate
<b>RDS</b>	Rate Determining Step
<b>SEM</b>	Scanning Electron Microscope
<b>SIMS</b>	Secondary Ion Mass Spectrometry
<b>STM</b>	Scanning Tunneling Microscopy/Microscope
<b>T</b>	Temperature
<b>TCD</b>	Thermal Conductivity Detector
<b>TDS</b>	Thermal Desorption Spectroscopy
<b>TEM</b>	Transmission electron microscopy
<b>TPO</b>	Temperature Programmed Oxidation
<b>UPS</b>	Ultraviolet Photoelectron Spectroscopy
<b>XPS</b>	X-ray Photoelectron Spectroscopy
<b>XRD</b>	X-ray Diffraction

## List of Schemes

<i>Scheme (1)</i>	<i>Reaction network (products and byproduct) in the dehydrogenation of ethylbenzene. Toluene and benzene are formed by (1) dealkylation reaction, (2) Hydrodealkylation reaction, (3) steam dealkylation, the Coke formation and gasification with steam are also shown in (4).....</i>	<i>4</i>
<i>Scheme (2)</i>	<i>Schematic of the life cycle of styrene catalyst with potassium and no other promoter additives as found from in-situ and ex-situ characterization work on the working catalyst by Muhler et. al[74]...</i>	<i>10</i>
<i>Scheme (3)</i>	<i>Schematic drawing of the catalytic oxidative dehydrogenation over carbon nanofilaments, (1) adsorption of ethylbenzene, (2) dehydrogenation at basic centers, (3) desorption of styrene, (4) adsorption of oxygen and reaction with oh groups, (5) desorption of water.....</i>	<i>13</i>
<i>Scheme (4)</i>	<i>An illustrative scheme for the main and side reaction pathways of the dehydrogenation of EB over the unpromoted Fe<sub>2</sub>O<sub>3</sub> model catalyst.....</i>	<i>116</i>
<i>Scheme (5)</i>	<i>An illustrative scheme explaining the role of water in preventing the reduction of the catalyst and the gasification of carbon deposits.....</i>	<i>117</i>
<i>Scheme (6)</i>	<i>(a) The main and side reaction pathways over the potassium promoted iron oxide model catalyst. (b) The role of water in the gasification of carbon deposits and the acceleration of potassium loss</i>	<i>118</i>

## **List of Figures**

<i>Figure 2.1</i>	<i>p(O<sub>2</sub>)-T phase diagram of the iron-oxygen system. The ranges where Fe<sub>3</sub>O<sub>4</sub> (A) and Fe<sub>2</sub>O<sub>3</sub> (B) films were grown on Pt (111) are indicated.....</i>	<i>16</i>
<i>Figure 2.2</i>	<i>Perspective side views of iron oxide crystal structures and top views cut parallel to the close packed oxygen layers. Bulk truncated (111) and (0001) surface structures terminated by outermost iron planes are shown. The surface unit cells are indicated. The top views are drawn with the full cation and anion sizes. In the side views the ionic radii were reduced by a factor of two.....</i>	<i>20</i>
<i>Figure 2.3</i>	<i>Structure models and layer arrangement for the ternary compound K<sub>2</sub>Fe<sub>22</sub>O<sub>34</sub> (a) and KFeO<sub>2</sub> (b). K is the large gray balls, O is the small dark balls and the Fe atoms are located in the center of the octahedral and the tetrahedral.....</i>	<i>22</i>
<i>Figure 2.4</i>	<i>LEED patterns at E=60 eV and top views of the corresponding surface structures of the different iron oxide films grown onto Pt(111). The unit cells in real and reciprocal space and the crystallographic directions in the cubic (a-c) and hexagonal crystal structures (d) are indicated. The epitaxial relationships between the oxide films and the substrate surface lattice are reflected in this figure.....</i>	<i>25</i>
<i>Figure 2.5</i>	<i>a)AES spectra of epitaxial iron oxide films grown onto Pt(111). (1) a-Fe<sub>2</sub>O<sub>3</sub>(0001), (2) the Fe<sub>3</sub>O<sub>4</sub>(111) before reaction, (3)</i>	



	<i>Fe<sub>3</sub>O<sub>4</sub>(111) after reaction and (b) KFe<sub>x</sub>O<sub>y</sub> films are at least 100 Å thick.....</i>	27
Figure 2.6	<i>Energetic and structural results for EB (filled symbols) and St (open symbols) adsorption on different substrate films. (a) Desorption energies from TDS [28] for chemisorbed (g) and physisorbed (b) species and adsorbate arrangement at low coverages of the initially adsorbing species (b on FeO, g on the others). Shown is adsorbed EB, the arrangement for St is similar. Adsorbate structure for Fe<sub>x</sub>O<sub>y</sub> from NEXAFS measurements [11]. The arrangement on K<sub>x</sub>Fe<sub>22</sub>O<sub>34</sub> is hypothetical. (b) Dependence of the desorption energy for the initially adsorbing species on the position of the first iron layer relative to the first oxygen layer.....</i>	28
Figure 2.7	<i>Mass spectrometer traces for EB and St under low pressure reaction conditions as indicated over poorly ordered and well ordered Fe<sub>2</sub>O<sub>3</sub> samples. Water was admitted at t=0. The traces reflect the periods of EB admission.....</i>	32
Figure 2.8	<i>Mass spectrometric analysis of a batch reactor experiment at intermediate pressure conditions as indicated for three Fe<sub>2</sub>O<sub>3</sub> model catalysts with differing surface quality. (1) well ordered, (2) intermediate order, (3) poorly ordered.....</i>	32
Figure 3.1	<i>Experimental setup, schematic, consisting of the preparation and analysis chamber (TDS) (1), PEEM (2) working at ultrahigh vacuum and the reactor chamber (3), working at pressures up to 1 bar. The sample on its support (figure 3) is moved by a magnetically coupled transfer rod. The transfer between the rod and the manipulator (M) or the reactor is accomplished by wobble sticks.....</i>	37
Figure 3.2	<i>a) Schematic side view of the magnetic transfer rod, the wobble stick, and the heating-cooling station in the transfer position, b) Front view photograph of the sample heating-cooling station on the manipulator.....</i>	38
Figure 3.3.	<i>A side view of the high pressure reaction cell with the flow reactor located inside. The sample is transferred fro UHV chamber using magnetic transfer line. With the help of wobblestick the sample is transferred and placed inside the reactor down in the chamber.....</i>	40
Figure 3.4	<i>Stagnation point micro-flow reactor for model catalysis at high pressure. 1: sample on sapphire support; 2: reactor cap; 3: fiber rods for coupling in laser irradiation; 4: thermocouple feed-through. (a) during insertion of the sample on a wobble stick, reactor cap withdrawn. (b) reactor cap closed, gas admission and analysis lines are schematically shown.....</i>	41
Figure 3.5	<i>The gas supply system used for the investigation of the styrene synthesis reaction carried out over iron oxide based catalysts in the presence of steam. All tubes are 1/16 inch in diameter. Helium (5.0) is used as carrier gas. The helium passes a 0.5 μm filter located directly in front of mass flow controllers (Bronkhorst).....</i>	43
Figure 3.6	<i>Schematic representation of the preparation of epitaxial iron oxide</i>	

	<i>films <math>Fe_xO_y</math> and <math>KFe_xO_y</math> on Pt(111), accomplished by repeated cycles of iron deposition and subsequent oxidation.....</i>	45
Figure 3.7	<i>a) The pressed hematite (<math>Fe_2O_3</math>) powder samples in form of pellets. b) A side view of the pressed pellet (1) mounted on a sapphire sample support with the help of Pt clamps (2) designed for this purpose, the thermocouple is mounted on the Pt holder. c) A heating homogeneity test for the sample holder using a laser source at 890K.....</i>	47
Figure 4.1.	<i>Time dependence of the St conversion rate at 870 K, normal conditions, EB and <math>H_2O</math> in the feed, over (a) <math>\alpha</math>-<math>Fe_2O_3(0001)</math>. The labels A-C give the positions where sample characterization was performed (see table (4.1)).....</i>	53
Figure 4.2.	<i>STM images of unpromoted <math>Fe_2O_3</math> model catalyst surface a) before, b) after 3 hours from reaction at normal reaction conditions, with the height profile along the indicated lines of each image is shown below.....</i>	55
Figure 4.3.	<i>Time dependence of the St conversion rate at 870 K, normal conditions, EB and <math>H_2O</math> in the feed, over <math>Fe_3O_4</math>. The label D and E give the position where sample characterization was performed (see table (4.2)).....</i>	56
Figure 4.4.	<i>Time dependence of the St conversion rate at 870 K, reductive conditions, EB and He in the feed, over <math>Fe_2O_3</math>. The labels F and G give the position where sample characterization was performed (see table (4.3)).....</i>	58
Figure 4.5	<i>AES spectrum of <math>Fe_2O_3</math> model catalyst after reaction at 870 K, reductive conditions, EB and He in the feed. Position G in Fig. (4.4).....</i>	59
Figure 4.6	<i>Time dependence of the St conversion rate at 870 K, oxidative conditions, EB, <math>H_2O</math> and <math>O_2</math> in the feed, over <math>Fe_2O_3</math>. The label H gives the position where sample characterization was performed (see table (4.4)).....</i>	60
Figure 4.7	<i>a) Conversion dependence of the St conversion rate at 870 K, oxidative conditions, EB, <math>H_2O</math> and <math>O_2</math> in the feed, over <math>Fe_2O_3</math> on EB/<math>O_2</math> molar ratio which is changed at the position labeled by numbers (1) 1:0.05, (2) 1:0.3, (3) 1:0.13, (4) 1:0.3 and (5) 1:0.13. b) Dependence of the steady state rate after 50 min of reaction at constant <math>O_2</math>/EB molar ratio(<math>r_{50}</math>). The dotted line is the estimated <math>O_2</math>/EB molar ratio which is theoretically needed to stabilize the high initial St conversion (see chapter 5).....</i>	62
Figure 4.8	<i>Deactivation dependence of the St conversion rate at 870 K, oxidative conditions, EB, <math>H_2O</math> and <math>O_2</math> in the feed, over <math>Fe_2O_3</math> after switching <math>O_2</math> on and off. The label I and J give the position where sample characterization was performed (see table (4.5)). For comparison, the deactivation when starting with a well ordered <math>Fe_2O_3</math> without <math>O_2</math> in the feed (from Fig. (4.1)) is shown in (a).....</i>	64
Figure 4.9	<i>The dependence of the St conversion rate at, oxidative conditions,</i>	

	<i>EB, H<sub>2</sub>O and O<sub>2</sub> in the feed, over Fe<sub>2</sub>O<sub>3</sub>.....</i>	66
Figure 4.10	<i>Time dependence of the St conversion rate at 870 K, normal conditions, EB and H<sub>2</sub>O in the feed, over KFe<sub>x</sub>O<sub>y</sub> with a (<math>I_K/I_{Fe} \sim 2.2</math>). The lower cure shows the St conversion rate over unpromoted Fe<sub>2</sub>O<sub>3</sub> for comparison.....</i>	67
Figure 4.11	<i>Time dependence of the St conversion rate at 870 K, normal conditions, EB and H<sub>2</sub>O in the feed, over KFe<sub>x</sub>O<sub>y</sub> with a) (<math>I_K/I_{Fe} \sim 0.9</math>), b) (<math>I_K/I_{Fe} \sim 4.2</math>).....</i>	69
Figure 4.12	<i>The build-up of carbon deposits over the unpromoted Fe<sub>2</sub>O<sub>3</sub> and potassium promoted (KFe<sub>x</sub>O<sub>y</sub>) catalyst (<math>I_K/I_{Fe} \sim 2.7</math>), expressed by the intensity ratios of the main Auger peaks of carbon to iron (<math>I_C/I_{Fe}</math>) with time on stream (normal conditions).....</i>	71
Figure 4.13	<i>Time dependence of the St conversion rate at 870 K, normal conditions, EB and H<sub>2</sub>O in the feed, over a potassium promoted (KFe<sub>x</sub>O<sub>y</sub>) with (<math>I_K/I_{Fe} \sim 2.2</math>), a) before reactivation with water, b) after reactivation with water for ~15 min.....</i>	73
Figure 4.14	<i>Time dependence of the St conversion rate at 870 K, oxidative conditions, EB, H<sub>2</sub>O and O<sub>2</sub> in the feed, over a potassium promoted (KFe<sub>x</sub>O<sub>y</sub>) model catalyst with (<math>I_K/I_{Fe} = 0.9</math>).....</i>	75
Figure 4.15	<i>Time dependence of the St conversion rate at 870 K, normal conditions, over KFe<sub>x</sub>O<sub>y</sub> with (<math>I_K/I_{Fe} = 1.9</math>), after 2 hrs H<sub>2</sub>O was switched, and the reaction is run under reductive conditions .....</i>	77
Figure 4.16	<i>Conversion dependence of the St conversion rate at 870 K, oxidative conditions, EB, H<sub>2</sub>O and O<sub>2</sub> in the feed, over a KFe<sub>x</sub>O<sub>y</sub> (<math>I_K/I_{Fe} \sim 2.7</math>) after switching O<sub>2</sub> off and on. B) Conversion dependence of the St conversion rate at 870 K, oxidative conditions, EB, H<sub>2</sub>O, and O<sub>2</sub> in the feed, over KFe<sub>x</sub>O<sub>y</sub> (<math>I_K/I_{Fe} \sim 2.7</math>), on EB/O<sub>2</sub> ratio, (1) 1:0.5, (2) 1:0.3, (3) 1:0.13 and (4) 1:0.3 and (5) 1:0.5. ....</i>	79
Figure 4.17	<i>The dependence of the St conversion rate at, oxidative conditions, EB, H<sub>2</sub>O and O<sub>2</sub> in the feed, over a KFe<sub>x</sub>O<sub>y</sub> (<math>I_K/I_{Fe} \sim 2.8</math>) on reaction temperature .....</i>	80
Figure 4.18	<i>Time dependence of the rate of St production (molecules. s<sup>-1</sup>. cm<sup>-2</sup> BET surface) over pressed pellets of Fe<sub>2</sub>O<sub>3</sub> powder in a fixed bed reactor. Reaction temperature 895 K, atmospheric pressure. : 1) EB/H<sub>2</sub>O = 1:6, 2) EB/H<sub>2</sub>O/O<sub>2</sub> = 1:6:0.4. In region A the GC measurement was switched from fast FID analysis to the combined FID-TCD method. This caused a shift in the baseline.....</i>	81
Figure 4.19	<i>SEM-EDX the pressed Fe<sub>2</sub>O<sub>3</sub> powder of unused samples (a) and (b). (c) carbon contaminated part. (e) and (f) after cleaning treatment for 30 min.....</i>	84
Figure 4.20	<i>a) St conversion over the pressed powder Fe<sub>2</sub>O<sub>3</sub> pellets used in the micro flow reactor at the same conditions like the model catalysts of 870 K and EB and H<sub>2</sub>O in the feed (normal conditions). b) XRD spectrum of the powder sample after reaction. The asterisk mark the positions of Fe<sub>3</sub>O<sub>4</sub> related diffraction peaks.....</i>	87
Figure 4.21	<i>SEM and EDX of the powder sample after reaction with EB and H<sub>2</sub>O</i>	

	<i>in the feed. The dashed line separates the red from the black parts of the sample.....</i>	86
Figure 4.22	<i>SEM and EDX of the powder sample after reaction with EB and H<sub>2</sub>O in the feed. The back was black (Fe<sub>3</sub>O<sub>4</sub>). The Image (b) shows also small 0.1 μm particles.....</i>	89
Figure 4.23	<i>SEM and EDX of the black part of the powder sample after reaction with EB and H<sub>2</sub>O in the feed (normal conditions). showing clearly the carbon deposits after reaction.....</i>	90
Figure 4.24	<i>SEM and EDX of the black part of the powder sample after reaction with EB and H<sub>2</sub>O in the feed normal conditions).....</i>	91
Figure 4.25	<i>a) St conversion over the pressed powder Fe<sub>2</sub>O<sub>3</sub> pellets used in the micro-flow reactor at the same conditions like the model catalyst of 870 K and EB and water in the feed, normal conditions. b) in the presence of oxygen in the feed, oxidative conditions,.....</i>	92
Figure 4.26	<i>SEM and EDX of the powder sample after reaction with EB and H<sub>2</sub>O in the feed. The sample was red (Fe<sub>2</sub>O<sub>3</sub>) and the EDX spectra shows that the surface is almost clean from the carbon deposits.....</i>	94
Figure 4.27	<i>SEM and EDX of the powder sample after reaction with EB and H<sub>2</sub>O and O<sub>2</sub> in the feed, oxidative condition).....</i>	95
Figure 4.28	<i>SEM and EDX of the powder sample after reaction with EB and H<sub>2</sub>O in the feed, oxidative conditions.....</i>	96
Figure 5.1	<i>Initial St conversion rate <math>r_{in}</math> ad time constant for deactivation <math>\tau_{de}</math> for samples with different initial K-content in terms of the Auger peak height ratio <math>I_K/I_{Fe}</math>. The composition where the ordered (2X2) structure is formed is indicated.....</i>	104
Figure 5.2	<i>Temperature dependence of the rate of styrene formation over the unpromoted and potassium promoted iron oxide model catalysts.....</i>	107
Figure 5.3	<i>EB dehydrogenation mechanism over the defects sites on the unpromoted (Fe<sub>2</sub>O<sub>3</sub>) [54]. Step 4 was found not to happen in case of reaction in presence of water alone. A side reaction (reduction of the Fe<sub>2</sub>O<sub>3</sub> to Fe<sub>3</sub>O<sub>4</sub>) also occurs.....</i>	109
Figure 5.4	<i>Reaction mechanism proposed by Muhler et. al. [74] proposed reaction mechanism for the dehydrogenation of EB to St over potassium promoted iron oxide catalysts.....</i>	109
Figure 5.5	<i>Comparison of the EDX C-K intensity peak between pressed powder samples after different treatments. The unused fresh pressed powder is also shown for comparison. The spectra are normalized to equal Fe-L intensity.....</i>	112

## List of Tables

Table 3.1	<i>Partial pressures and molar ratios of reactive gases in the gas feed for the used standard reaction conditions. The rest to the working pressure of 1 bar is He. The standard reaction temperature is 870 K, the standard total flow 25 ml min<sup>-1</sup>.....</i>	46
Table 4.1	<i>LEED patterns and intensity ratios of the main Auger peaks of carbon, oxygen and iron before and after reaction for the unpromoted Fe<sub>2</sub>O<sub>3</sub> model catalysts.....</i>	54
Table 4.2	<i>LEED patterns and intensity ratios of the main Auger peaks of carbon, oxygen and iron before and after different treatments for the unpromoted Fe<sub>3</sub>O<sub>4</sub> model catalysts.....</i>	56
Table 4.3	<i>LEED patterns and intensity ratios of the main Auger peaks of carbon, oxygen and iron before and after reaction (reductive conditions) for the unpromoted Fe<sub>2</sub>O<sub>3</sub> model catalysts.....</i>	58
Table 4.4	<i>LEED patterns and intensity ratios of the main Auger peaks of carbon, oxygen and iron for the unpromoted Fe<sub>2</sub>O<sub>3</sub> model catalysts before and after reaction with water and oxygen in the feed.....</i>	60
Table 4.5	<i>LEED patterns and intensity ratios of the main Auger peaks of carbon, oxygen and iron for the unpromoted Fe<sub>2</sub>O<sub>3</sub> model catalysts after oxygen on - off experiments (Fig. (4.8a,b)).....</i>	65
Table 4.6	<i>LEED patterns and intensity ratios of the main Auger peaks of carbon, oxygen, potassium and iron before and after reaction with EB and H<sub>2</sub>O in the feed (normal conditions) for the promoted (KFe<sub>x</sub>O<sub>y</sub>) model catalysts with different K-loading.....</i>	70
Table 4.7	<i>LEED patterns and intensity ratios of the main Auger peaks of carbon, oxygen, potassium and iron before and after reaction with EB and H<sub>2</sub>O in the feed for the promoted KFe<sub>x</sub>O<sub>y</sub> model catalysts effect of reactivation with steam.....</i>	72
Table 4.8	<i>LEED patterns and intensity ratios of the main Auger peaks of carbon, oxygen, potassium and iron before and after reaction with EB and H<sub>2</sub>O in the feed for the promoted KFe<sub>x</sub>O<sub>y</sub> model catalysts with (<math>I_K/I_{Fe} \sim 2.8</math>), before and after reactivation with water for 15 min</i>	74
Table 4.9	<i>LEED patterns and intensity ratios of the main Auger peaks of carbon, oxygen, potassium and iron before and after reaction with EB, H<sub>2</sub>O and O<sub>2</sub> in the feed (oxidative conditions) for the promoted KFe<sub>x</sub>O<sub>y</sub> model catalysts with (<math>I_K/I_{Fe} = 1.0</math>).....</i>	75
Table 4.10	<i>LEED patterns and intensity ratios of the main Auger peaks of carbon, oxygen, potassium and iron before and after reaction with EB and H<sub>e</sub> in the feed over the promoted KFe<sub>x</sub>O<sub>y</sub> model catalysts.....</i>	77